5.1 Introduction

Crystallization is a thermally activated process in amorphous solids. The crystallization of metallic glasses typically occurs by two independent but inter-correlated elementary events, i.e., nucleation and growth, each of them being controlled by either mechanisms: diffusion of atoms to, through, or out of the liquid or glassy matrix crystal interface and surface chemical reaction i.e., incorporation of reacting units into and out of the interface. Nucleation is a rapid process as compared to growth. Nucleation may be homogeneous or heterogeneous, or there may be pre- existing nuclei of various natures. Growth may be primary, eutectic or polymorphic [5.1-5.2]. Crystallization studies of metallic glasses are of importance in understanding mechanisms of phase transformations far from equilibrium, evaluating the glass forming ability (GFA) of the melts and producing ultrarefined microstructure [5.3-5.5]. The study of crystallization process of metallic glass forming alloys is important in understanding amorphization in metallic systems. The kinetics of crystallization must be known to attain products with required fraction crystallized or to avoid the degradation of materials when they are cooling from high processing temperatures. The kinetics of the solid state phase transformations can be studied using thermal analysis techniques such as differential scanning calorimetry (DSC). To analyze the data obtained from DSC and hence to determine the kinetic parameters of the crystallization processes (say, activation energy, rate constant etc.), raise two important issues: (i) the selection of the mode of experiment (isothermal or non-isothermal) and, (ii) the choice of a sound method for the

analysis of the experimental data. Crystallization process can be investigated under isothermal and non-isothermal conditions. Non-isothermal experiments can be performed more easily and faster than isothermal experiments. Moreover, they provide smaller noise-to-signal ratio for kinetic experiments [5.6]. So to study crystallization process under non-isothermal condition various approximation and theoretical models have been proposed [5.7-5.11]. For the kinetic analysis of the crystallization process under non-isothermal condition, the choice of a reliable method is very important.

The analysis of data procured from DSC experiments can be done in two ways, isokinetic and iso conversional. A single value of kinetic parameters such as activation energy is obtained by isokinetic methods, since they assume the transformation mechanism to be same throughout the temperature or time range. On the other hand, an isoconversional method assumes the transformation mechanism at a constant degree of conversion as a function of temperature and provides kinetic parameters varying with the degree of conversion, α. Generally, multi-component metallic glasses crystallize in multiple steps so their transformation mechanism cannot be considered to be the same throughout the process. Different mechanisms may be involved for different steps. Thus, selection of correct method to study crystallization behavior of metallic glasses is a major issue. Many researchers [5.12-5.15] have studied crystallization kinetics by various isokinetic and isoconversional methods. Recently, Lu and Li [5.16] have used various isokinetic and isoconversional methods for studying the kinetics of non-isothermal crystallization in Cu-based metallic glasses. Some

others researchers, such as Wu et al. [5.17] and Svoboda and Malek [5.18], have considered that isoconversional methods are sufficient for the study of crystallization kinetics.

To understand the relative importance of isokinetic methods and isoconversional methods in the present work second crystallization event of $Zr_{52}Cu_{18}Ni_{14}Al_{10}Ti_6$ metallic glass is analyzed by both the methods to obtain value for the activation energies of crystallization as well as other kinetic parameters.

5.2 Theoretical Formulation

5.2.1 Theory of Phase Transformation

Most of the methods, developed to study the phase transformations involving nucleation and growth, are depend on the transformation rate equation given by [5.19-5.23], Kolmogorov, Johnson, Mehl and Avrami (KJMA) equation. KJMA equation is used to characterize the crystallization kinetics and crystallization mechanism in isothermal conditions [5.24]. The KJMA rate equation is given by

$$\frac{d\alpha}{dt} = nk(1-\alpha)[-\ln(1-\alpha)]^{(n-1)/n} \tag{5.1}$$

where, α is the degree of transformation at a given time t, *n* is Avrami (growth) exponent and *k* is the rate constant.

The Arrhenius form of the rate constant is given by

$$k(T) = k_0 \exp\left(-\frac{E}{RT}\right) \tag{5.2}$$

where, k_0 pre-exponential factor, $E \rightarrow$ activation energy, and $R \rightarrow$ universal gas constant

KJMA rate equation is often extended to non-isothermal conditions. However, KJMA equation can be used to describe non-isothermal and isothermal transformation only if the entire nucleation process takes place very early during the crystallization process and thereafter the growth is dependent on temperature and does not on the thermal history. KJMA rate equation is based on some important assumptions and it has been suggested that the KJMA kinetic equation is accurate for reactions with linear growth subject to several conditions [5.25].

5.2.2 Iso-conversional methods

For non iso-thermal crystallization kinetics the reaction rate can be expressed by the following kinetic equation [5.26]:

$$\frac{d\alpha}{dT} = \frac{1}{\beta} k(T) f(\alpha) = \frac{k_0}{\beta} \exp\left(-\frac{E}{RT}\right) f(\alpha) \qquad (5.3)$$

where, $k(T)$ is rate constant, β is heating rate, α is degree of conversion, and $f(\alpha)$ is the reaction model. The determination of kinetic parameters k_o, E and $f(\alpha)$ is the chief aim of studying kinetics of crystallization.

Isoconversional methods are independent of reaction model $f(\alpha)$, and hence they are also known as model free methods. The isoconversional methods require the knowledge of temperatures $T_\alpha(\beta)$ at which an equivalent stage of reaction occurs for various heating rates. The equivalent stage is defined as the stage at which a

fixed amount is transformed or at which a fixed fraction, α of the total amount is transformed [5.27]. Further, model free methods are classified as linear and non-linear isoconversional methods. The linear methods can be further divided into integral and differential methods. The linear integral isoconversional methods depend on the approximation of the temperature integral. The differential isoconversional methods depend on the rate of transformation at $T_\alpha(\beta)$. Vyazovkin [5.28] introduced a non-linear isoconversional method to increase the accuracy of evaluating the activation energy.

Separation of variables and integration of equation (5.3) gives:

$$g(\alpha) = \int_0^\alpha [f(\alpha)]^{-1} = \frac{k_0}{\beta} \int_0^T \exp\left(-\frac{E}{RT}\right) dT \tag{5.4}$$

Above integral equation doesn't have an exact analytical solution, hence various approximations of this integral are suggested in literature [5.29-5.33], for evaluation of activation energies dependent on the degree of conversion, α. Starink [5.31] has analyzed and discussed various iso-conversional methods in terms of their applicability and limitations.

5.2.2.1 Linear Integral Isoconversional Methods

[a] *Kissinger-Akahira-Sunose (KAS) method*

To evaluate the temperature integral in eq. (5.4), Kissinger-Akahira-Sunose (KAS) [5.7,5.34] used the approximation given by Coats and Redfern [5.35], and hence derived the following equation:

$$\ln\left(\frac{\beta}{T_\alpha^2}\right) = -\frac{E_\alpha}{RT_\alpha} + \ln\left(\frac{k_0 R}{E_\alpha}\right) \tag{5.5}$$

The activation energy can be evaluated from the slope of plot $ln(\beta/T^2)$ vs $1000/T$ for constant conversion, α. The discussion given ahead describes some of the methods available in the literature which are basically special cases of the KAS.

i) Kissinger method: Kissinger equation is based on the assumption that the rate of reaction is highest at peak temperature (T_p). It calculates activation energy at a constant degree of conversion, α i.e., at $T_\alpha = T_p$ only. The equation used by Kissinger is

$$\ln\left(\frac{\beta}{T_p^2}\right) = -\frac{E}{RT_p} + \ln\left(\frac{k_0 R}{E}\right) \tag{5.6}$$

The slope and intercept of the ln (β/T_p^2) vs. $1000/T_p$ plot, gives the values of activation energy, E and the pre-exponential factor (k_0) respectively. k_o is the frequency factor i.e. the number of jumps required by an atom to overcome the barrier and form stable nuclei. This method is independent of reaction order and has very less dependence on the thermal history of the material.

ii) Augis & Bennett's method: This method is a modification of Kissinger equation in which peak temperature (T_p) along with onset temperature of crystallization (T_o) is used [5.36]. This method is applicable to heterogeneous reactions.

$$\ln\left(\frac{\beta}{\left(T_p - T_o\right)}\right) = -\frac{E}{RT_p} + \ln\left(k_0\right) \tag{5.7}$$

where T_p and T_o are the peak and the onset temperatures of crystallization respectively. The values of E is obtained from the plot $(ln(\beta/(T_p-T_o))$ vs $1000/T_p$.

iii) Boswell method: Boswell method [5.37] was formulated to overcome the limitations of Augis and Bennett method. As $((T_p-T_0)/T_p) \approx 1$, Augis and Bennett methods may provide crude results. Boswell method determines the activation energy at peak temperature using the following equation

$$\ln\frac{\beta}{T_p} = -\frac{E}{RT_p} + const \tag{5.8}$$

[b] *Ozawa-Flynn-Wall (OFW) method*

In OFW [5.38-5.39] method Doyle's approximation [5.40-5.42] is used to simplify the temperature integral in eq. (5.4) which is approximated to be equal to (-E/RT):

$$\ln\beta = -1.0516\frac{E(\alpha)}{RT_\alpha} + const \tag{5.9}$$

The factor 1.0516 is a correction factor.

The plot of $ln\beta$ vs $1000/T_\alpha$ gives the slope $-1.0516\ E(\alpha)/R$ from which the activation energy has been evaluated. At $T_\alpha = T_p$ (peak temperature), above equation reduces to Ozawa method and the value of E is also determined.

5.2.2.2 Linear Differential Isoconversional Method

[a] *Friedman method*

Friedman [5.43] derived an expression for estimation of activation energy of crystallization based on the differential of the transformed fraction. The expression given by Friedman is as follows:

$$\ln\left(\frac{d\alpha}{dt}\right)_{\alpha} = \ln\beta\left(\frac{d\alpha}{dT}\right)_{\alpha} = -\frac{E_{\alpha}}{RT_{\alpha}} + \ln\left(k_0 f(\alpha)\right) \tag{5.10}$$

The values of E_α calculated from the slope of the plot ln (β (dα/dT)$_\alpha$) vs. 1000/T_α for constant conversion, α. Since this method does not take any mathematical approximation for the temperature integral, it is considered to give accurate estimate of E. Thus the method does not require any assumption on $f(\alpha)$, i.e. it is a so-called model-free method. However, being a differential method, its accuracy depends upon signal noise.

[b] *Gao and Wang method*

A special case of Friedman method, which involves the determination of E only at T_p was suggested by Gao & Wang [5.44]. This model is based on the assumption of random nucleation and site saturation. The expression used by Gao & Wang is as follows:

$$\ln\left(\beta\frac{d\alpha}{dT_p}\right) = -\frac{E}{RT_p} + const \tag{5.11}$$

The values of E can be calculated from the slope of the plot ln (β (dα/dT_p)) vs. 1000/T_p.

5.2.3 Isokinetic methods

These methods are model fitting methods that depend upon the consideration of various kind of models for the determination of kinetic parameters E and k_0. Isokinetic methods are, in general, employed to study the kinetics of phase transformations occurring in isothermal conditions. These methods rely on the isokinetic hypotheses to separate the kinetics of the transformation from its dependence on temperature.

The isokinetic methods are mainly based on the Kolmogorov-Johnson-Mehl-Avrami (KJMA) rate equation [5.45-5.49] which is described by eq. (5.1) & eq.(5.2).

From equations (5.1) & (5.2) transformed fraction can be expressed as

$$\alpha = 1 - \exp\left[-\frac{k_0}{\beta} \int_{T_0}^{T} \exp\left(-\frac{E}{RT} \right) dT \right]^n \tag{5.12}$$

The integral in eq. (5.12) does not have an exact solution and hence one has to switch to approximations. Various approximations have been used in literature to obtain an accurate solution of the integral [5.50-5.52].

On employing Gorbachev approximation [5.52] i.e., eq. (5.13) in eq. (5.12) we obtain eq. (5.14).

$$\int_0^T e^{-E/RT} dT = \frac{RT^2}{E+2RT} e^{-E/RT} \tag{5.13}$$

$$\alpha = 1 - \exp\left[-\left\{ \frac{k_0 RT^2}{\beta(E+2RT)} \exp\left(-\frac{E}{RT} \right) dT \right\}^n \right] \tag{5.14}$$

The values of E, n and k_0 can be determined by fitting the experimental data of α to eq. (5.14) with the help of method of least square. Different isokinetic methods are described below:

[a] *Matusita and Sakka method*

Matusita and Sakka [5.53] gave the following expression for studying the non isothermal crystallization kinetics of metallic glasses.

$$\ln[-\ln(1-\alpha)] = -n \ln \beta - \frac{mE}{RT} + Const \tag{5.15}$$

where the integer m defines the dimensionality of the crystal and the Avrami exponent n gives information about the nucleation process. The value of n can be obtained from the slope of the plot of ln[-ln(1-α)] versus lnβ, at a constant temperature. Further, the slope of the plot ln[-ln(1-α)] versus 1000/T at a constant heating rate gives the value of m.

Further, for the nonisothermal crystallization, the local Avrami exponent can be calculated from the following equation [5.54]:

$$n(\alpha) = -\frac{R}{E(\alpha)} \frac{d(\ln(-\ln(1-\alpha)))}{d(1/T)} \tag{5.16}$$

[b] *Modified Kissinger method*

The modified Kissinger [5.55] equation is expressed as:

$$\ln\left(\frac{\beta^n}{T_p^2}\right) = -\frac{mE}{RT_p} + Const \tag{5.17}$$

where E is the activation energy for crystallization, T_p is the peak temperature, R is the universal gas constant and m is known as the dimensionality of growth. The slope of $\ln(\beta^n/T_p^2)$ versus $1000/T_p$ gives the value of activation energy of crystallization. In this approach, the determination of the parameters m and n becomes important for determination of E.

5.2.4 Testing techniques

For testing the applicability of the KJMA model under non-isothermal conditions, different pre-examined tests have been suggested by Henderson [5.56] and Malek [5.57-5.58]. The first method is an investigation of a straight line in the plot of ln[-ln(1-α)] vs. 1/T. Linearity of this graph was the most popular testing method for the validity of KJMA kinetics. However it has been proved to be unreliable.

5.2.4.1 Malek Test

A simple and practical test has been given by Malek [5.57] for checking the validity of KJMA model in non-isothermal conditions in which two functions y(α)

and z(α) are calculated. The dependence of y(α) and z(α) on α can be expressed as below:

$$y(\alpha) = \phi \exp(E/RT) \tag{5.18}$$

$$z(\alpha) = \phi T^2 \tag{5.19}$$

Where φ is the heat flow evaluated during the crystal growth, represented by the following equation

$$\phi = \Delta H_c k_0 \exp(-E/RT) f(\alpha) \tag{5.20}$$

and $$f(\alpha) = n(1-\alpha)\left[-\ln(1-\alpha)\right]^{(n-1)/n} \tag{5.21}$$

where, ΔH_c is the enthalpy difference associated with crystallization process. The maximum of $y(\alpha)$ and $z(\alpha)$ are represented by α_M and $\alpha_{p.}$

If $0 < \alpha_M < \alpha_P$, and α_P is not equal to zero, then the equation for $f(\alpha)$ given by Sestak-Berggren can be used for evaluating the kinetic parameters. Sestak-Berggren (S-B) [5.59] equation is given as:

$$f(\alpha) = \alpha^M (1-\alpha)^N \tag{5.22}$$

Where, M and N are kinetic parameters, their ratio can be calculated as:

$$\frac{M}{N} = \frac{\alpha_M}{(1-\alpha_M)} \tag{5.23}$$

Considering S-B equation, the reaction rate can be given as:

$$\frac{d\alpha}{dt} = Z\exp\left(-\frac{E_\alpha}{RT}\right)\alpha^M(1-\alpha)^N \tag{5.24}$$

Another way of representing S-B equation is:

$$\ln\left[\left(\frac{d\alpha}{dt}\right)\exp\left(\frac{E_\alpha}{RT}\right)\right] = \ln Z + N\ln\left[\alpha^{M/N}(1-\alpha)\right] \tag{5.25}$$

The value of N can be obtained from the slope of the plot $\ln[(d\alpha/dt)\exp(E_\alpha/RT)]$ versus $\ln[\alpha^{M/N}(1-\alpha)]$. Then, the parameter M can be calculated from equation (5.23). After calculating value of M and N, S-B equation is obtained. Then the so obtained $f(\alpha)$ is used to plot the master curve.

5.2.4.2 Master plot method

In order to check the established reaction model i.e. JMA and SB model "Master plot" method is employed. In master plot method [5.60], the $f(\alpha)$ is calculated at α=0.5, then theoretically calculated values of $f(\alpha)$ is reduced by dividing it by $f(0.5)$:

$$\frac{f(\alpha)}{f(0.5)} = \frac{d\alpha/dt}{(d\alpha/dt)_{0.5}}\frac{\exp(E_\alpha/RT)}{\exp(E_\alpha/RT_{0.5})} \tag{5.26}$$

The left hand side of eq. (5.26) represents the theoretical value of reaction model which is characteristic of each kinetic function. Whereas right hand side represents the experimental values obtained from DSC data if the apparent activation energy is known, and remains constant throughout the entire reaction. Comparison of both sides of eq. (5.26) determines which kinetic model describes the experimental reaction process.

5.2.4.3 Normalized heat flow curve

In order to check the match between the experimental and the theoretically derived normalized heat flow curves, the theoretical normalized heat flow curves are obtained from eq.(5.20) & (5.21), using calculated kinetic parameters *E* and *n*, to check the applicability of KJMA model.

5.3 Results and discussion

5.3.1 Crystallization kinetics of Zr based metallic glass

Since the discovery of Zr based metallic glasses, various efforts have been made to understand their GFA and thermal stability against crystallization. Many studies regarding the crystallization kinetics under isothermal and non-isothermal conditions, for Zr based metallic alloys are available in literature [5.61-5.67]. Qiao et al [5.68] have studied crystallization kinetics of $Zr_{55}Cu_{30}Ni_5Al_{10}$ metallic glass by isochronal and isothermal routes. Prashanth et al [5.69] investigated kinetics of $Zr_{65}Ag_5Cu_{12.5}Ni_{10}Al_{7.5}$ and showed that crystallization process is diffusion-controlled with three dimensional growth. Lu et al [5.70] studied the crystallization process of three clearly separated crystallization peaks of $(Zr_{46}Cu_{42}Al_7Y_5)_{95}Be_5$ by isoconversional, isokinetic and master plots methods. More recently, Kasyap et al have carried out crystallization kinetics of $Ti_{20}Cu_{60}Zr_{20}$ metallic glass using isoconversional methods by modulated DSC [5.71]. The aim of this study is to analyze the second crystallization event of Zr based metallic glass and to obtain accurate values for the activation energies of crystallization as well as other kinetic parameters. It is important to study

variation of activation energy, *E* with degree of crystallization as it provides useful information about the different mechanism involved in the transformation process.

In order to confirm the elemental composition of $Zr_{52}Cu_{18}Ni_{14}Al_{10}Ti_6$ amorphous ribbons, Energy Dispersive X-ray analysis (EDX) was performed. EDX scan of whole surface of the specimen gives an average composition of this alloy as shown in inset of fig 5.1. This value is close to the nominal composition $Zr_{52}Cu_{18}Ni_{14}Al_{10}Ti_6$.

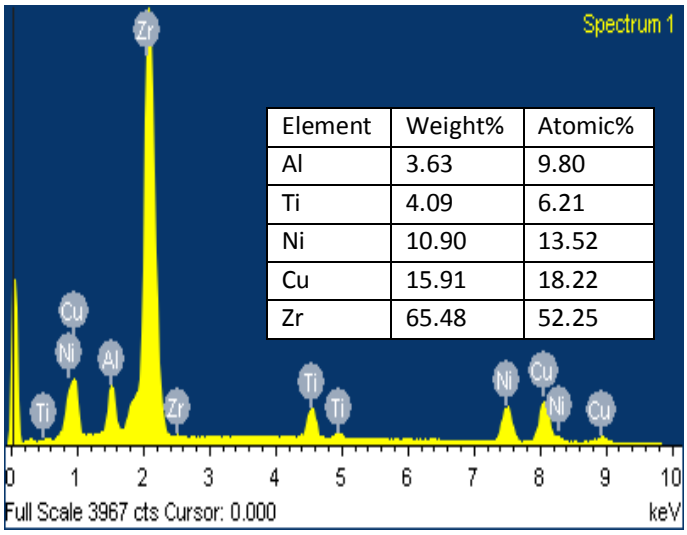

Element	Weight%	Atomic%
Al	3.63	9.80
Ti	4.09	6.21
Ni	10.90	13.52
Cu	15.91	18.22
Zr	65.48	52.25

Fig. 5.1: Energy Dispersive X-ray analysis (EDX) of $Zr_{52}Cu_{18}Ni_{14}Al_{10}Ti_6$ amorphous ribbons

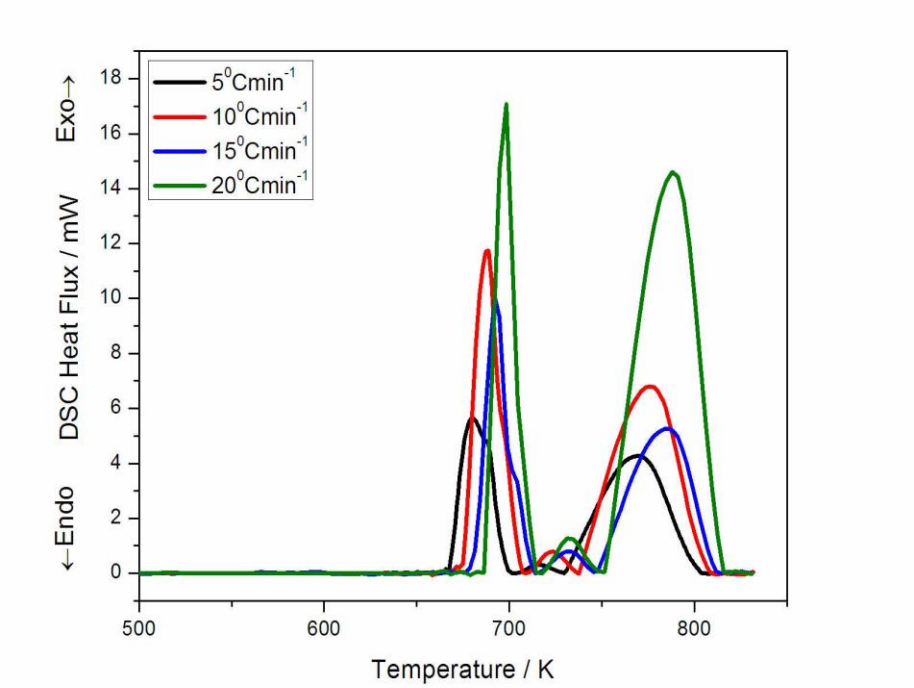

Fig. 5.2 DSC Thermogram for $Zr_{52}Cu_{18}Ni_{14}Al_{10}Ti_6$

Figure-5.2 shows the DSC thermograms for $Zr_{52}Cu_{18}Ni_{14}Al_{10}Ti_6$ at four different heating rates (5, 10, 15, 20 deg/min). It can be observed that crystallization occurs in two steps. The first and second peaks of crystallization correspond to low temperature and high temperature respectively. As heating rate increases the peak shifts towards higher temperature, which implies that crystallization depends upon the heating rate during the continuous heating process. The second crystallization event is more sensitive towards heating rate as compared to first peak. Earlier Patel et al [5.72] have carried out the analysis of crystallization kinetics of $Zr_{52}Cu_{18}Ni_{14}Al_{10}Ti_6$ for the first peak by isokinetic and isoconversional methods. The analysis of the first peak revealed that the activation energy (E) initially increases slowly in the range α (=0.3-0.6) followed by a quick increase in E with α. This indicates that second crystallization step starts even before the first step is completed. This inspires us for the analysis of next crystallization event. Also in

order to understand the overall crystallization process, analysis of second peak is important. The second peak or crystallization event may have originated due to following reasons: (a) the nature of crystal produced during first crystallization is metastable. With increase in temperature these metastable material transform into another structure. (b) A multicomponent metallic glass does not crystallize in a single step. The crystal which persists within the melt is of different composition which crystallizes with a much slower kinetics to another phase at high temperature. (c) Some of the crystals formed during first crystallization are small and they grow to form larger grains. The calorimetric data of glasses cannot determine which of these occurrences are more favourable [5.73]. A sharp peak is observed for first crystallization event due to formation of nuclei at higher rate whereas for the second peak it is found to be broad as growth take place slowly. Also, a small peak is observed around 730K, at all heating rates. The intensity of this peak is very small as compared to the other two peaks. This less prominent peak may have occurred due to the overlapping of first and second peaks. This does not indicate any significant process. Hence we have analyzed only the prominent peaks. The crystallized fraction, α is calculated from DSC thermogram at different temperatures. The so obtained DSC data can be analysed by both methods i.e isokinetic and isoconversional.

5.3.2 Testing techniques to check the validation of different methods

Now to understand which method is more appropriate to study the second step crystallization process various testing techniques are carried out to fit

experimental data. Firstly to check the validation of JMA model experimental data of fractional crystallization is fitted by iterative least square fitting method using eq. (5.14). Initial estimate of E and k_0 are calculated from Kissinger equation.

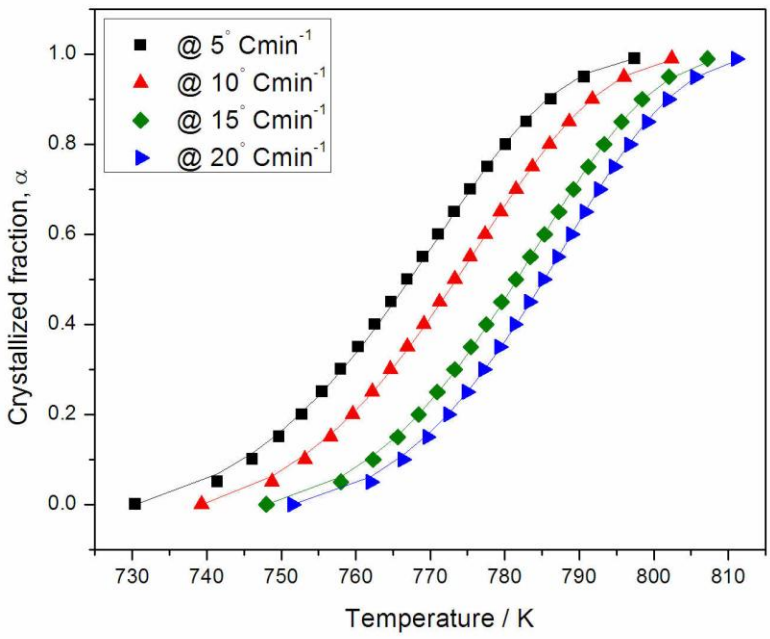

Fig.5.3 Variation of Crystallized fraction with temperature at different heating rate: symbols represent experimental points and solid lines show the least square fitted curve by eq. (5.14).

The sigmoidal shape of crystallized fraction with temperature represents the bulk crystallization and excludes the chance of surface crystallization [5.74]. The above sigmoidal curve represents three different stages of crystallization. In the intial stage only nucleation occurs and with further increase in reaction rates both nucleation and growth of nuclei takes place. Finally due to decrease in surface area nuclei start coalescing and hence reaction rate decreases. The perfect fitting of experimental data to eq. (5.14) confirms the validity of JMA model. Table 5.1

reports the value of n, k_o and E at different heating rate calculated by least square fitting method.

Table 5.1 Values of Avrami (growth) exponent (n), pre-exponential factor (k_0) and activation energy (E) obtained by least square fitting of fractional crystallization data for second crystallization peak

Heating Rates	**KJMA**		
	N	***k₀* (s^{-1})**	***E* ($kJmol^{-1}$)**
5	1.09	3.66×10^{15}	264
10	1.13	2.8×10^{15}	260
15	1.22	2.08×10^{15}	258
20	1.26	2.28×10^{15}	258

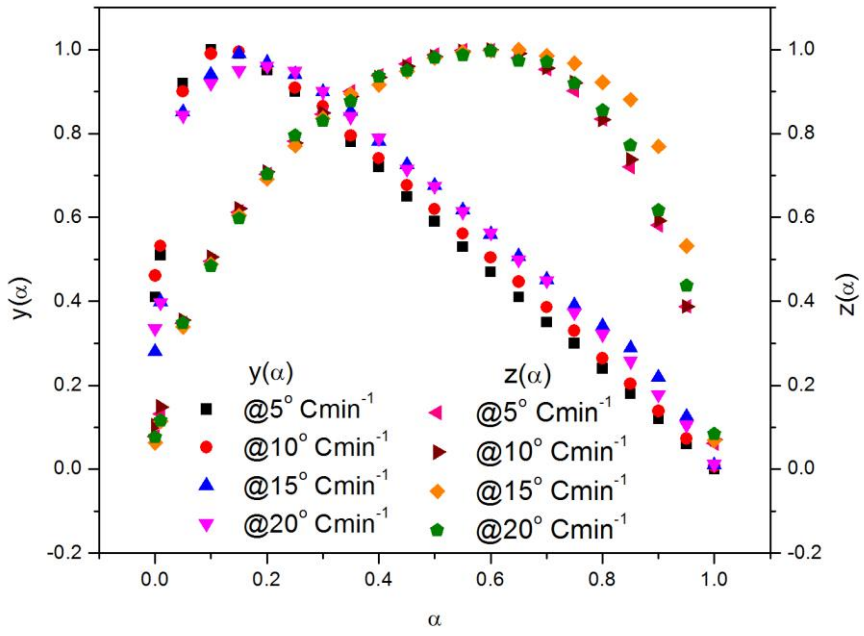

Fig.5.4 Normalized $y(\alpha)$ and $z(\alpha)$ with crystallized fraction α for different heating rates

According to Malek test, functions $y(\alpha)$ and $z(\alpha)$ are plotted as a function of α as shown in fig.5.4. In the present case we have calculated both $y(\alpha)$ and $z(\alpha)$ as expressed in eq.(5.18) and (5.19) respectively. The maximum of $y(\alpha)$ and $z(\alpha)$ are represented by α_M and α_p . According to Malek, KJMA model is valid if the maximum value of $z(\alpha)$ function i.e. α_P is confined to the interval $0.61 < \alpha_P < 0.65$. The present analysis shows that the peak of the plots of $z(\alpha)$ vs. α at different heating rates lie within the range 0.57 - 0.66. Thus, α_P fall in the proposed interval and hence KJMA model can be used to study the kinetic process.

Further the theoretical master plots are drawn by assuming the different kinetic models and compared with the experimental master plots which allow us to select the appropriate kinetic model that describes kinetics of crystallization.

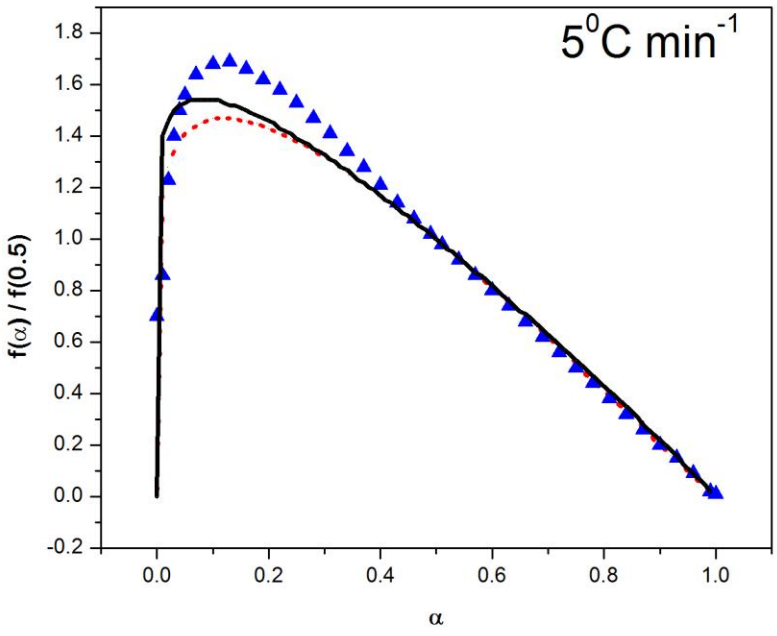

Fig. 5.5 Master plot at different heating rates; (▲▲▲)experimental, (—) JMA, (····) S-B: @5^0C/min

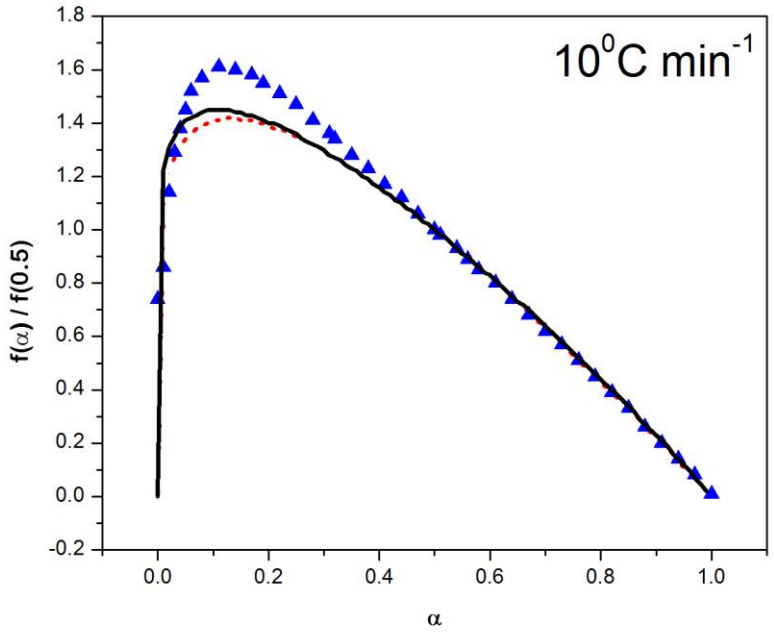

Fig. 5.6 Master plot at different heating rates; (▲▲▲)experimental, (—) JMA, (·····) S-B: @10^{0}C/min.

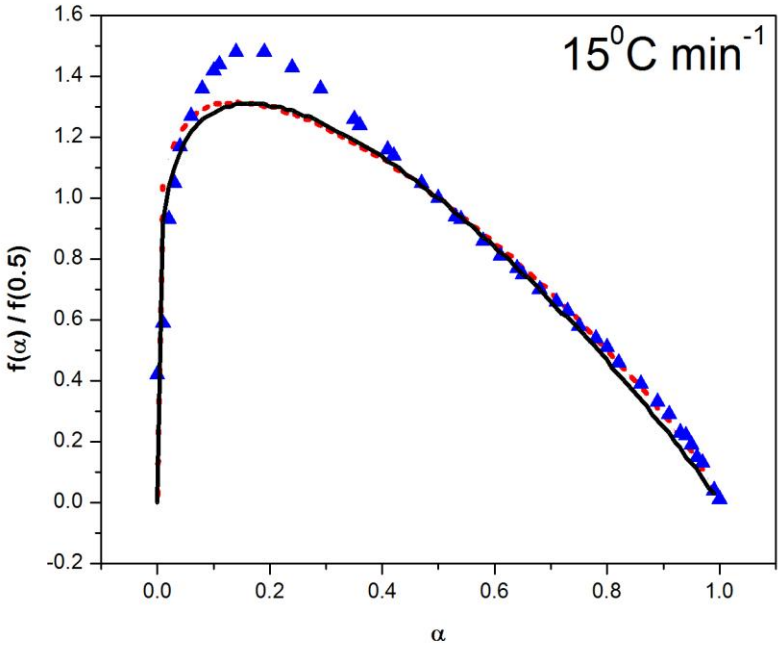

Fig. 5.7 Master plot at different heating rates; (▲▲▲) experimental, (—) JMA, (·····) S-B: @15^{0}C/min.

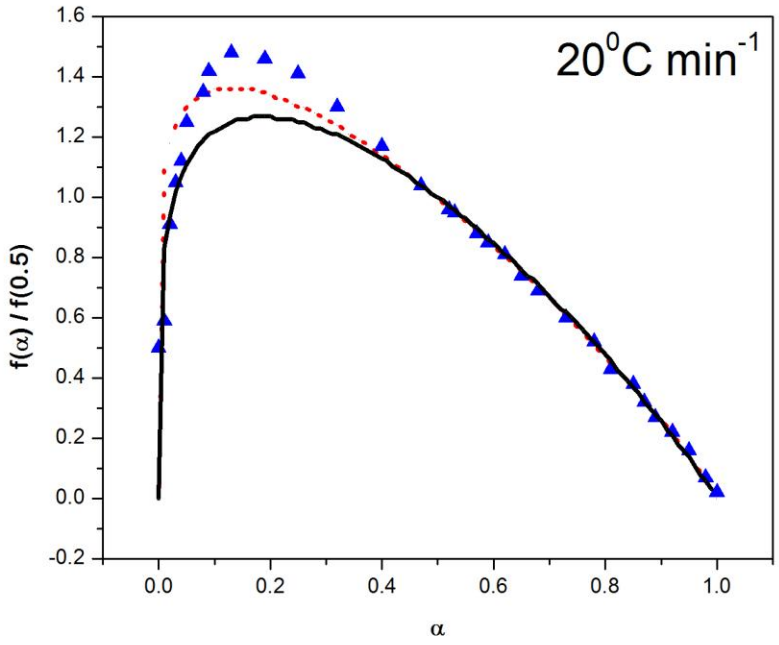

Fig. 5.8. Master plot at different heating rates; (▲▲▲)experimental, (—) JMA, (·····) S-B: @20^{0}C/min.

In non-isothermal conditions, the knowledge of both α as a function of temperature and activation energy is required for calculating the master plot curves from the experimental data. The Master plots represented by fig. 5.5 to fig.5.8 show the comparison between theoretical and experimental values of reduced $f(\alpha)$ with respect to $f(0.5)$. The trend followed by the theoretical models for all heating rate is same as the experimental results. The theoretical curves deviate from experimental curve at α=0.1. This deviation increases till α=0.2 and then it decreases. The deviation of theoretical S-B curves from experimental curve decreases with increase in heating rate while for JMA the deviation increases. At α=0.5 both curves match well with experimental curve till the end of the peak. Master plots confirm the validity of S-B model and JMA model for metallic glass.

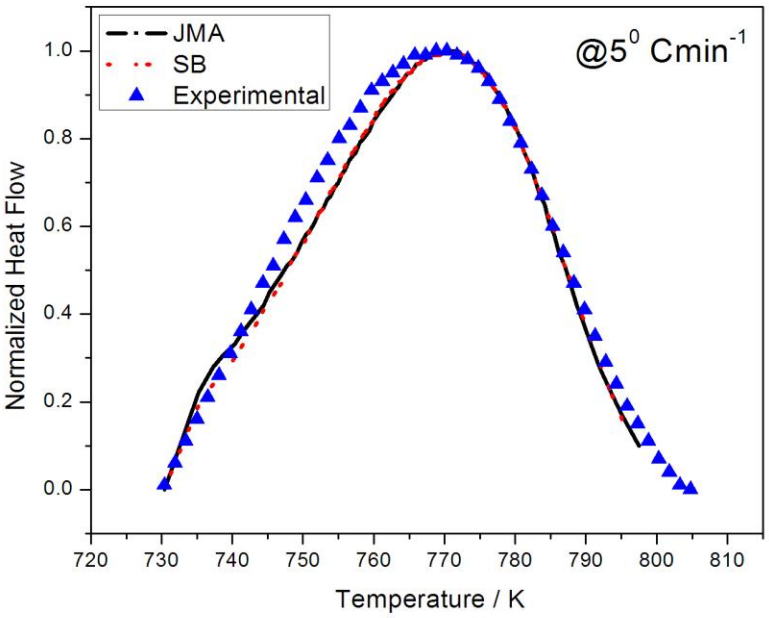

Fig. 5.9 Normalized heat flow curves at different heating rates @5^{0}C/min.

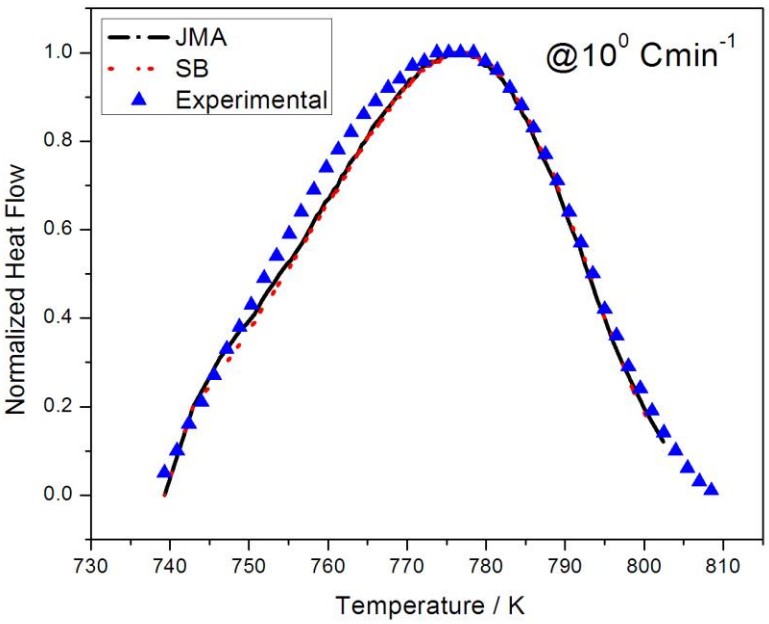

Fig. 5.10 Normalized heat flow curves at different heating rates @10^{0}C/min.

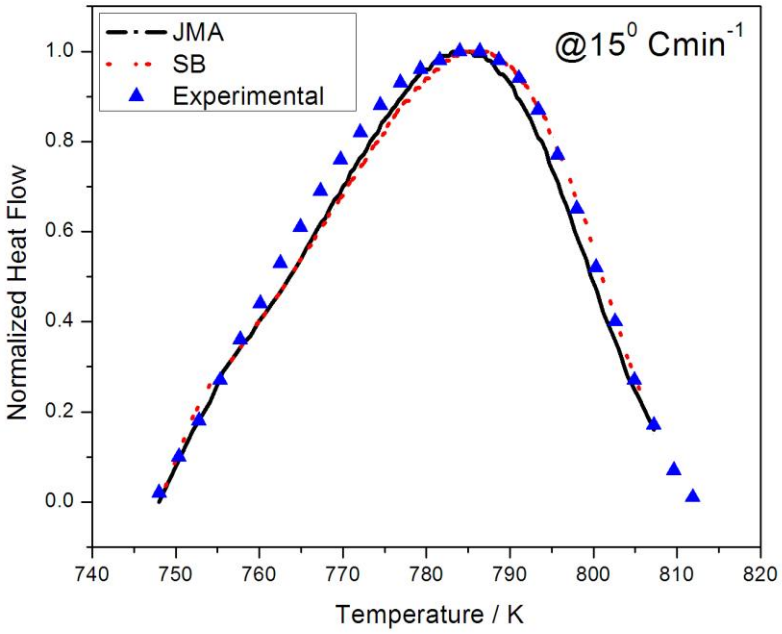

Fig. 5.11 Normalized heat flow curves at different heating rates @15^{0}C/min.

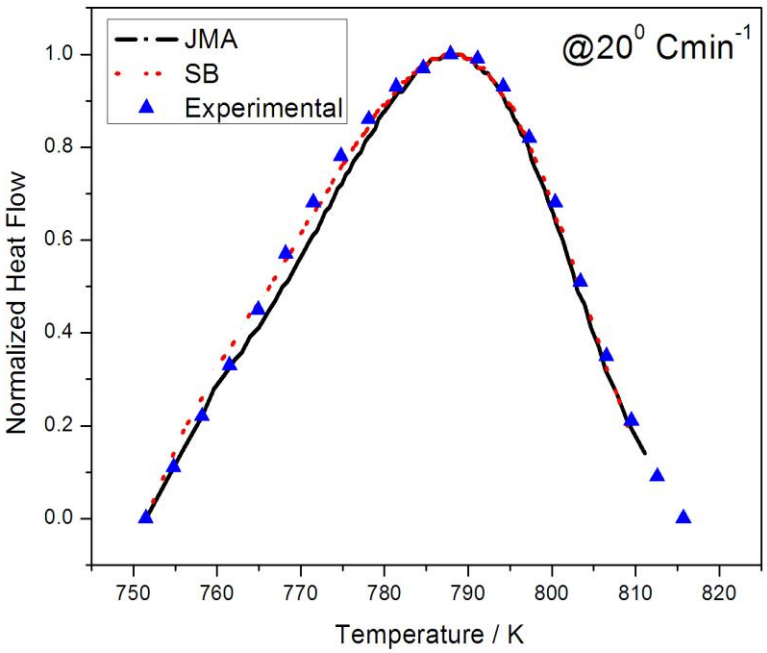

Fig. 5.12 Normalized heat flow curves at different heating rates @20^{0}C/min.

Fig. 5.9-5.12 shows the match between the theoretical and experimental heat flow curve. From fig. 5.9-5.12 it can be observed that at initial stage the theoretical heat flow curve matches with experimental data. Both the reaction models superimpose the experimental heat flow curve at peak temperature for all the heating rates. After peak, the theoretical model provides a fairly good agreement with experimental data. Therefore, a good match between the theoretical heat flow curves with experimental data indicate that the crystallization kinetics for Zr based system can be studied by both reaction models i.e KJMA and SB. As heating rate increases, the normalized heat flow curve obtained by SB reaction model exactly matches with the experimental data. Hence to study the crystallization process iso-kinetic methods are necessary. But, they provide single values of kinetic parameters, which is insufficient to understand entire crystallization process. So, iso-conversional method which gives *E* depending on α is important. Hence in the present case the crystallization kinetics is studied by both isokinetic and iso-conversional method.

5.3.3 Isoconversional methods

5.3.3.1 Linear integral iso-conversional methods

The activation energy at different extent of conversion (fractional crystallization) has been evaluated as shown in table 5.2 using the linear integral isoconversional methods given by KAS and OFW. It can be observed from table 5.2 that the *E* values obtained from both the methods increases with increase in α. Fig. 5.13 shows the plot for KAS method (eq.5.5) at α=0.7 and fig. 5.14-5.16 show the

plots for special cases of KAS method. Also fig. 5.17 shows the plot for OFW (eq. 5.9) method α=0.7.

Table 5.2 Local activation energies (E_α) at different degrees of conversions, α for different methods

α	E_α (kJ mol^{-1})		
	KAS	**OFW**	**Friedman**
0.1	265 ± 5	290 ± 5	328 ± 6
0.2	310 ± 6	307± 5	355 ± 6
0.3	322 ± 5	320 ± 5	356 ± 6
0.4	329 ± 6	327 ± 6	376 ± 6
0.5	346 ± 7	344 ± 7	394 ± 7
0.6	364 ± 7	360 ± 7	413 ± 7
0.7	381 ± 7	376 ± 6	439 ± 6
0.8	403 ± 8	398 ± 8	484 ± 7
0.9	448 ± 6	441 ± 7	531 ± 6

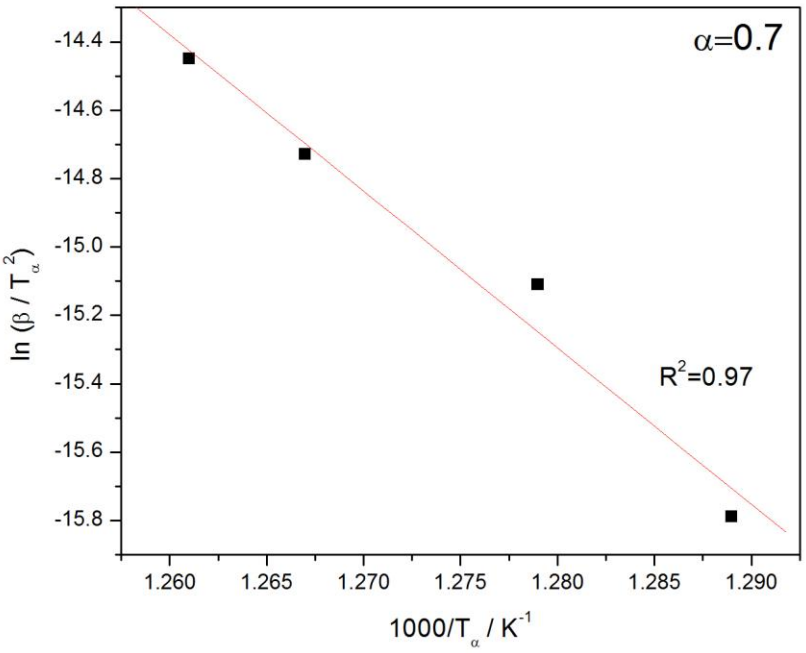

Fig. 5.13 KAS plot for α =0.7

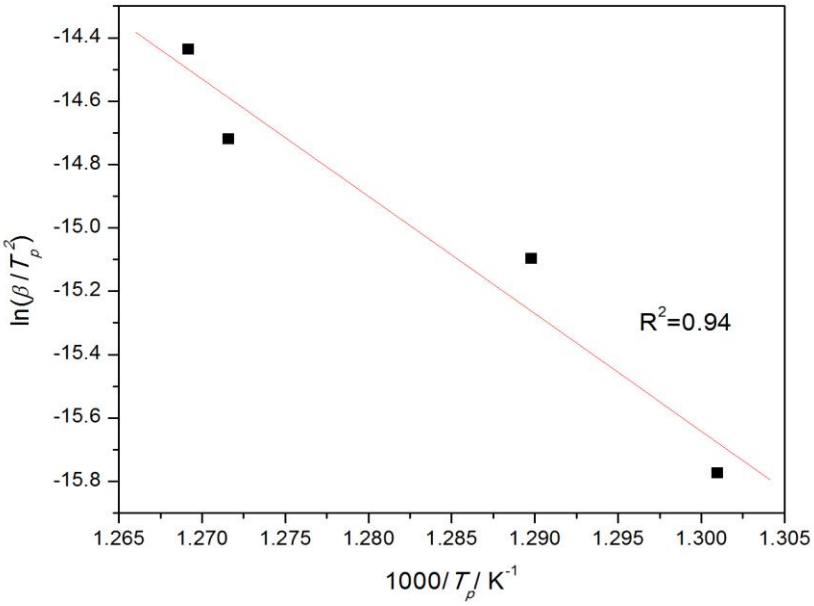

Fig. 5.14 Kissinger plot

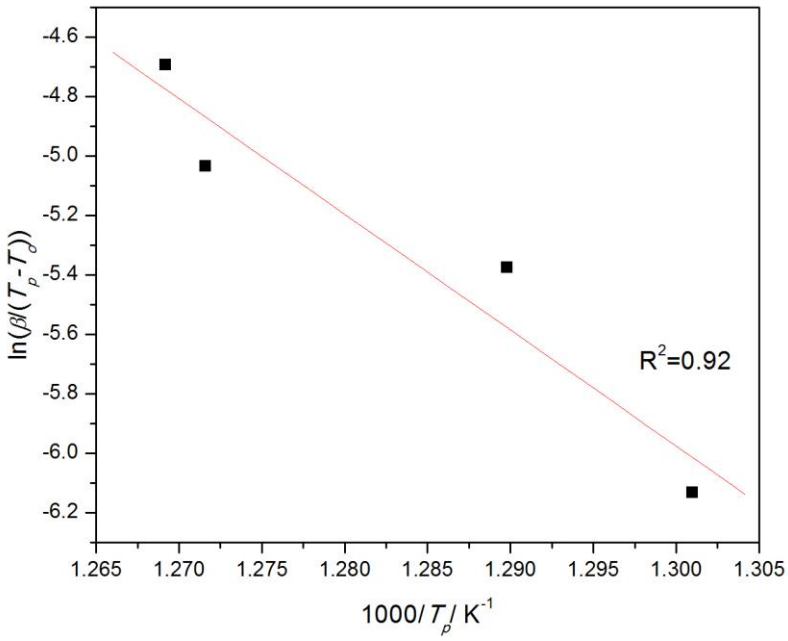

Fig.5.15 Augis & Bennett's plot

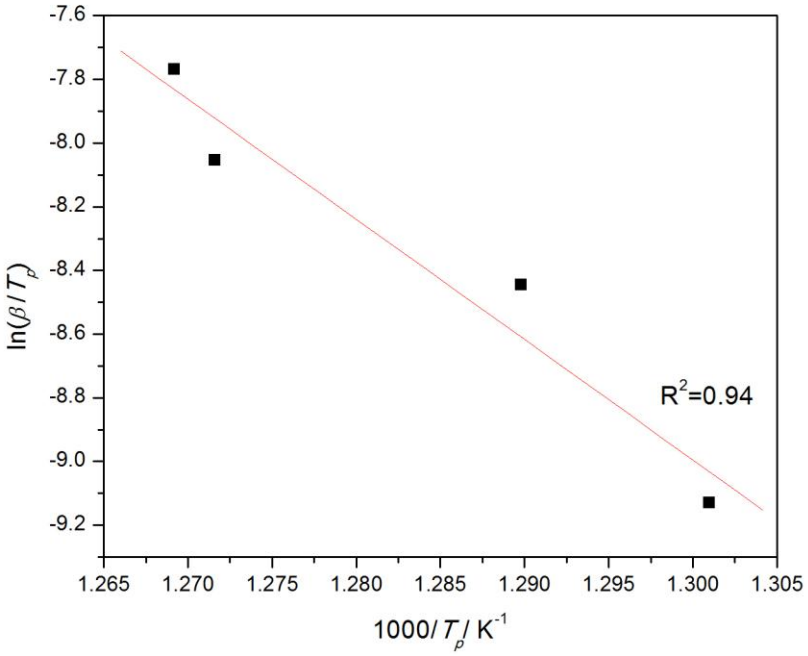

Fig. 5.16 Boswell plot

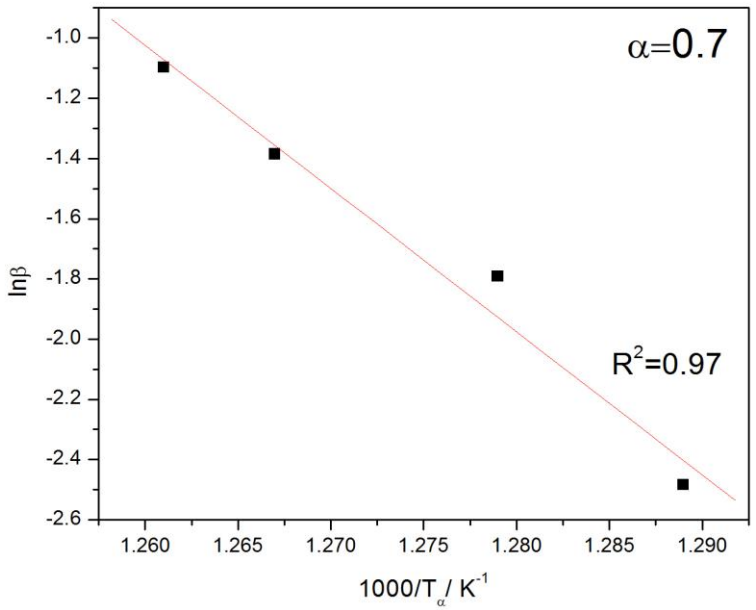

Fig. 5.17 OFW plot for α =0.7

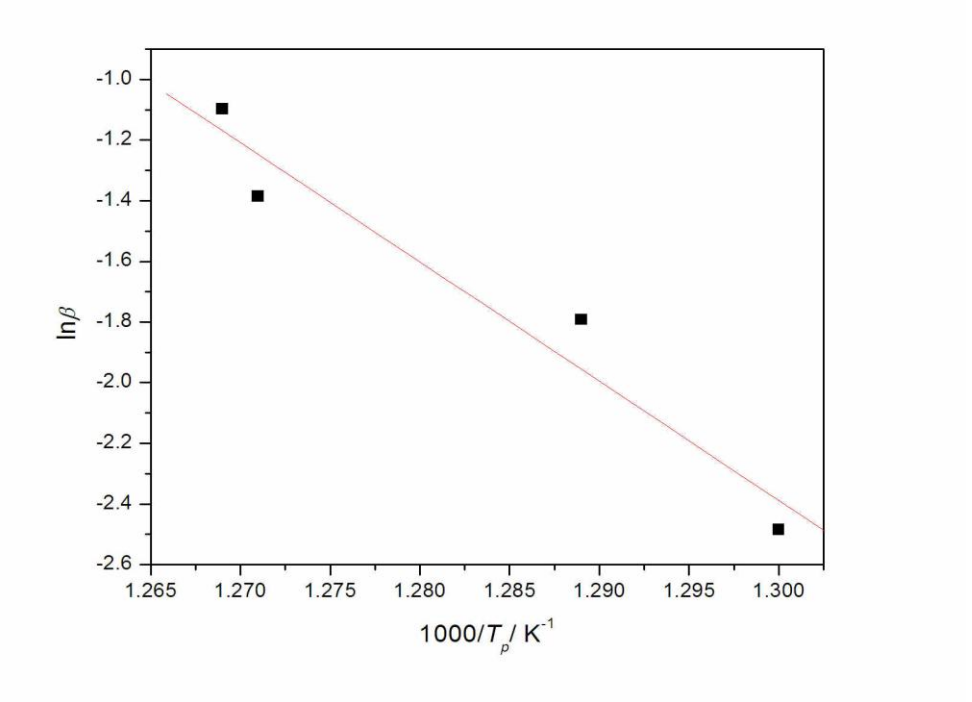

Fig. 5.18 Ozawa plot

Table 5.3 Activation energy (E) and pre-exponential factor (k_0) for different methods

Methods	***E* (kJmol^{-1})**	**k_0 (sec^{-1})**
Kissinger	308 ± 8	4.77 x 10^{15}
Augis & Bennett	324 ± 10	2.56 x 10^{19}
Boswell	314 ± 8	-
Ozawa	311 ± 8	-
Gao & Wang	357 ± 9	-

Table 5.3 reports the activation energy and pre-exponential factor by different isoconversional methods. The Kissinger method assumes that the reaction rate is maximum at the peak temperature (T_p) (table 5.3). This assumption implies a constant degree of conversion (α_p) at T_p. The values of activation energy listed in table 5.3 by different methods are the special cases of different method and most of them are calculated at peak temperature to know the maximum reaction rate.

5.3.3.2 Linear differential iso-conversional methods

The non-isothermal data obtained from thermograms recorded at several heating rates 5, 10, 15 and 20 deg/min^{-1}for Zr based metallic glass, the values of E_α is calculated as suggested by Friedmann from the slope of the plot ln (β (dα/dT)$_\alpha$) vs. 1000/T_α for constant conversion, α (Fig. 5.19), are given in table 5.2. The values of E calculated from the slope of these plots increases with the increase in crystallized fraction, α.

The activation energy obtained from the Gao and Wang plot of ln (β (dα/dT_p)) vs. 1000/T_p (Fig. 5.20) is given in table 5.3. This method gives a single value of E at the peak crystallization temperature. The deduced value of E = 357 kJ/mol., which is similar to other obtained values

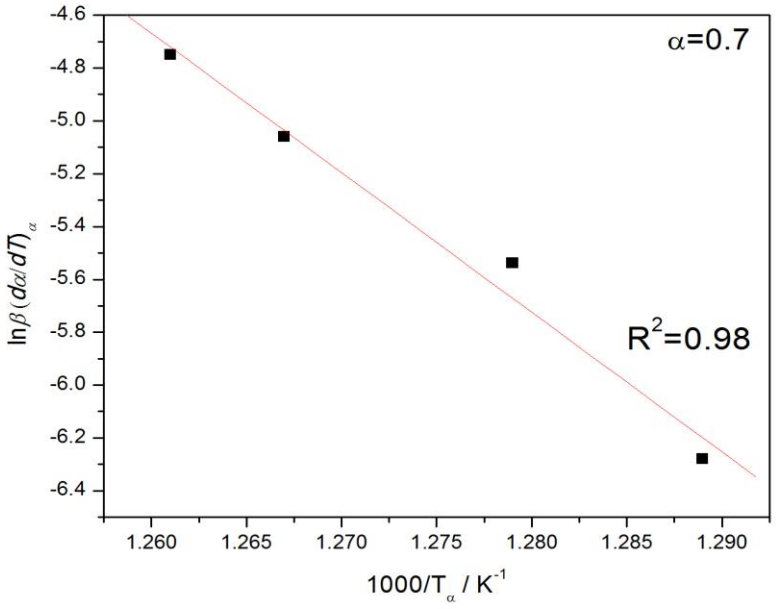

Fig. 5.19 Friedman plot for α =0.7

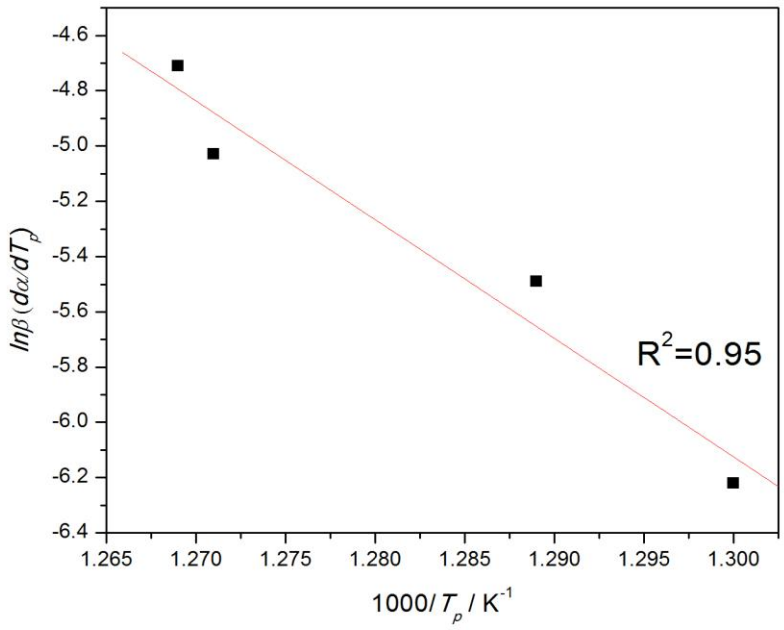

Fig.5.20 Gao & Wang plot

It is observed that *E* values for second step of crystallization are greater than that of first step, by all the models. This indicates that secondary crystallization requires more energy for overcoming the barrier and forming stable nuclei. In general it is observed that activation energy for first peak is higher compared to second peak [5.75-5.76], indicating that the primary phase transition has modified the matrix and secondary crystallization has become easier. But for the present case it is observed that activation energy for first peak [5.72] is lower than second peak. For $Co_{69}Fe_3Si_{18}B_{10}$ metallic glass [5.75], the values of E for first and second step are 370 and 327 $kJmol^{-1}$ respectively by Kissinger method. But for the present case, E values are found to be 259 and 308 $kJmol^{-1}$ for first and second peaks respectively. Also the activation energy increases rapidly for second peak.

For first peak it was found to increase from 264 to 303 $kJmol^{-1}$, whereas for second peak it increases from 265 to 448 $kJmol^{-1}$ by KAS method.

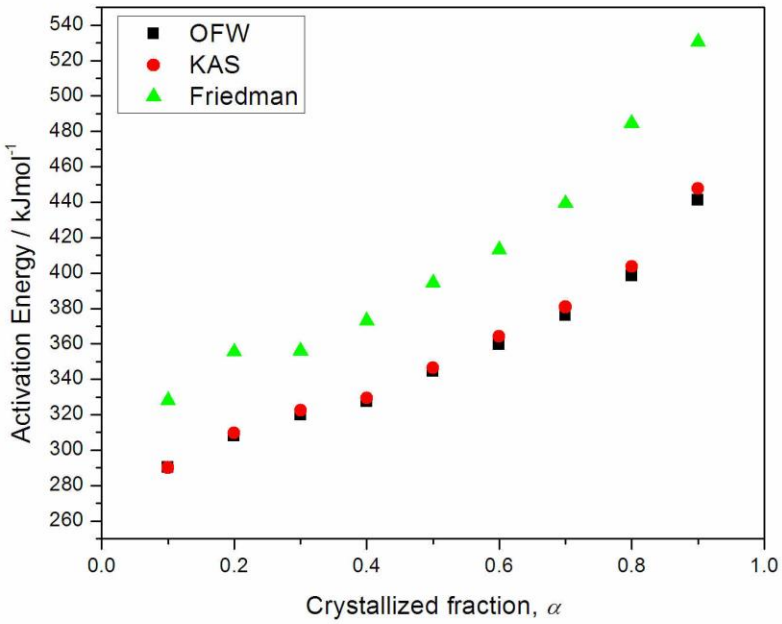

Fig. 5.21 Local activation energies (E_α) at different α from different methods

In the fig.5.21 variation of local activation energies (E_α) with crystallized fraction (α) for peak-2 is shown by three different methods i.e. KAS, OFW and Friedman. The value of activation energies are reported in the table- 5.2. It can be observed that values of E_α obtained by KAS and OFW methods lie close to each other. As observed from the fig. 5.21, the values of local activation energy of crystallization constantly increase with the crystallized fraction α. This increase in E_α may be understood in terms of decrease in free volume of crystal due to the presence of primary crystallites. The formation of secondary crystallite takes place on primary crystallites. For the growth of secondary crystallites the atoms are required to move through the melt which faces a barrier due to presence of primary

crystallites and decreasing free volume. As a result of which the activation energy E_α for secondary crystallization increases with increase in α, at a higher rate as compared to primary crystallization.

5.3.4 Isokinetic Methods

The Matusita and Sakka plot for a constant temperature, the plot of $ln[-ln(1-\alpha)]$ versus $ln\beta$ gives a straight line [Fig. 5.22] and the slope gives the value of n. Here we have taken seven different constant temperatures and the average value of n comes out to be 2.32. The plot of $ln[-ln(1-\alpha)]$ versus $1/T$ at constant heating rate should be a straight line and the value of m is obtained from the slope [Fig.5.23]. The value of m for second crystallization peak is 1.32. This implies that secondary crystallization proceed through one dimensional growth of nuclei. Table 5.4 represents the values of Avrami exponent (n) and dimensionality (m) calculated by Matusita and Sakka method. It can be noticed that the value of n increases with increasing heating rates, indicating a higher particle density at higher heating rates.

Table 5.4 Values of Avrami exponent (n) and dimensionality (m) by Matusita and Sakka method

Heating Rates	**Value of Avrami exponent (n)**	**Dimensionality (m)**
5	2.22	1.22
10	2.27	1.27
15	2.37	1.37
20	2.43	1.43

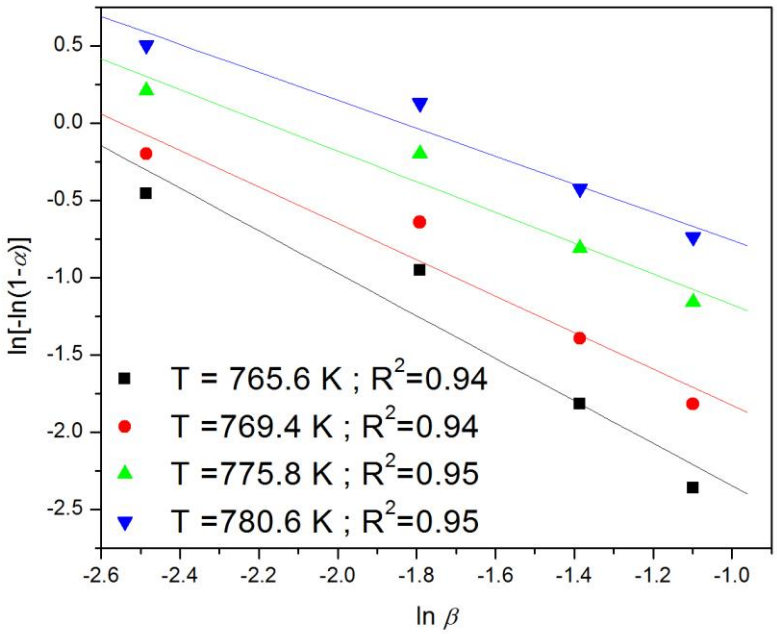

Fig.5.22 Plot of ln[-ln(1 - α)] vs. ln β

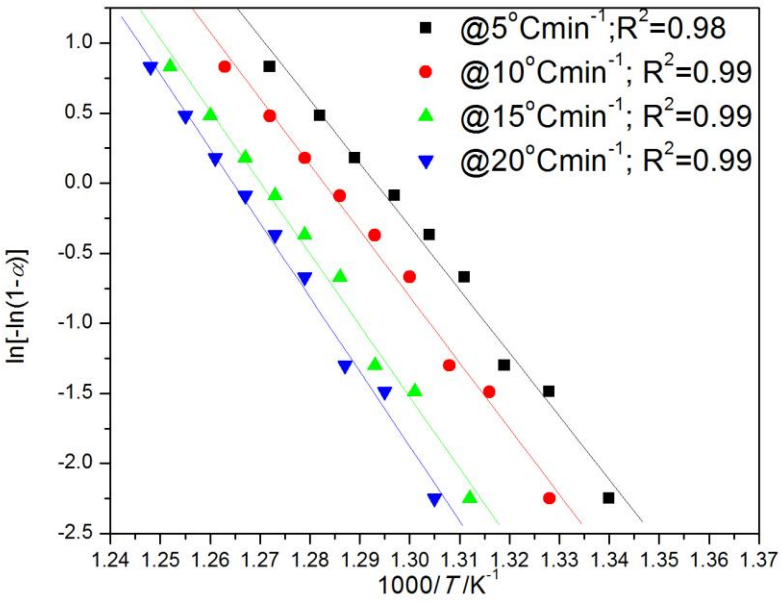

Fig. 5.23 Plot of ln[-ln(1 - α)] vs. 1000/T for different heating rates

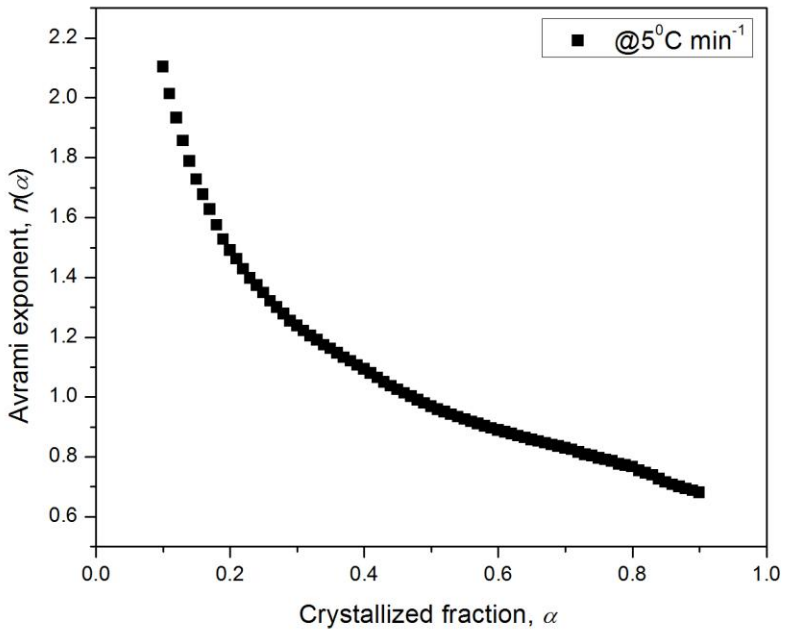

Fig.5.24 variation of local Avrami exponent with crystallized fraction

Fig. 5.24 represents the variation of local Avrami exponent with crystallized fraction at constant heating rate of 5^0C min^{-1}. It can be observed from this figure that the value of n (α) decreases with an increase in α, indicating that the transformation rate of crystalline particles decrease throughout the crystallization process. Similar behaviour is observed at all heating rates.

The modified Kissinger equation eq. (5.17) is utilized to derive the activation energy at peak temperature. In this equation, m is known as the dimensionality of growth. In this approach, the determination of the parameters m and n becomes important for determination of E. In order to derive E from this equation, one must know the value of n. Here $m=n$-1, and the value of n is obtained from

Matusita and Sakka method. Then plots of $\ln\left(\frac{\beta^n}{T_p^2}\right)$ Vs. $\frac{1}{T_p}$ (Fig. 5.25) gives the values of activation energy *E*, and the average *E* obtained is 269 kJ mol^{-1}.

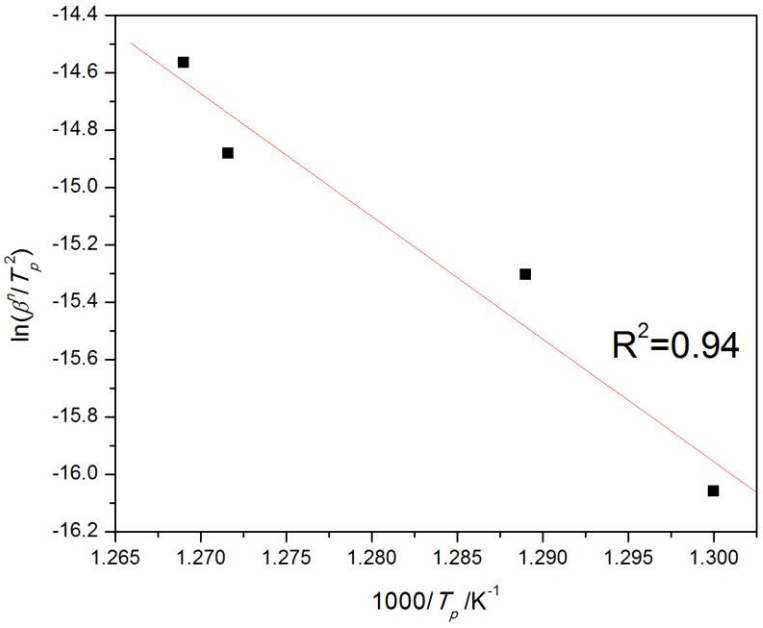

Fig.5.25 Modified Kissinger plot

5.3.5 Effect of heating rate on primary and secondary crystallization processes

Primary crystallization process for $Zr_{52}Cu_{18}Ni_{14}Al_{10}Ti_6$ metallic glass was analyzed by Patel et al. [5.72]. The value of Avrami growth exponent (n) was found to be 2.66, which indicates that surface crystallization occurs in primary step of crystallization process. In the second step of crystallization the value of Avrami exponent indicates diffusion controlled crystallization process.

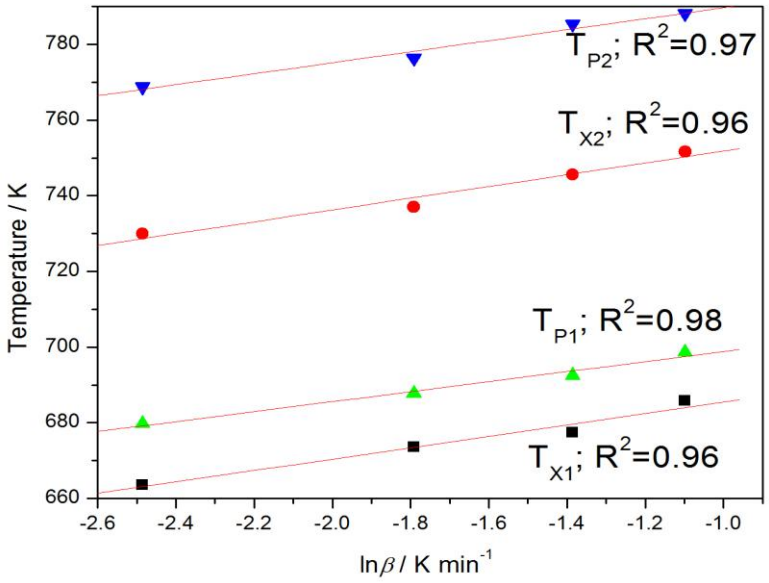

Fig 5.26 Relationship between temperature and ln β for T_{x1}, T_{x2}, T_{p1} and T_{p2}

Fig 5.26 shows the variation of characteristic temperatures i.e., onset and peak crystallization (T_x and T_p respectively) for peak 1 and peak 2, with heating rate.

Lasocka's relation [5.77] was used to study the relationship between temperature and heating rate.

$$T = A + B\ln\beta \qquad (5.27)$$

where A and B are constants.

Table 5.5 Values of A &B for $Zr_{52}Cu_{18}Ni_{14}Al_{10}Ti_6$ metallic glass

Constants	T_{x1}	T_{p1}	T_{x2}	T_{p2}
A	700 ± 4	712 ± 2	767 ± 4	804 ± 3
B	15 ± 2	13 ± 1	16 ± 2	14 ± 2

Least square method was used to obtain the values of A and B. The value of B indicates sensitivity towards heating rate. The values of constants A & B are reported in table-5.5. From the table it can be observed that the value of slope for peak-2 i.e secondary crystallization is greater than primary crystallization. The value of B for T_{x2} is largest, whereas it is smallest for T_{p1}. Hence secondary crystallization is more sensitive towards heating treatment.

5.4 Conclusion

The second peak in thermogram which represents secondary crystallization was investigated to understand complete crystallization process. A reaction model independently proposed by Kolmogorov -John-Mehl-Avrami (KJMA) is found to be the most suitable for describing the nucleation and growth process during the non-isothermal crystallization of metallic glasses. This model does help to determine the kinetic parameters, like the dimensionality of growth (apart from *E* and *A*). A criterion given by Malek and master plot method suggests that JMA model is applicable for kinetic studies. Further, normalized heat flow curve were examined to check the validity of JMA & SB models for studying kinetic process. The results indicate that both models lie in close agreement with experimental data at higher heating rates. Since, to understand the entire crystallization process the information of value of *E* at different α is necessary, both routes for studying non-isothermal crystallization were followed.

The non isothermal crystallization kinetics for $Zr_{52}Cu_{18}Ni_{14}Al_{10}Ti_6$ metallic glass was studied by both isokinetic and iso-conversional methods. Isokinetic methods

provide the single value of activation energy E with Avrami exponent that gives the dimensionality of crystal growth. Isoconversional methods provide the activation energy E_α depending on different values of α. Hence crystallization which is complex process can be well understood by both methods. Different kinetic parameters obtained by both methods for studying crystallization kinetics provide good result in the entire range. All the methods satisfactorily explains the the variation of E_α with α. The activation energies obtained by KAS, OFW and Friedman shows an increasing trend with α. The increase of E_α with α may be due to decrease in free volume, which provides hindrance in diffusion of atoms towards stable configuration. The value of Avrami exponent decreases with α, indicating decrease in nucleation rate. The sensitivity of the characteristic temperatures towards heating rate is more for secondary crystallization event as compared to the primary crystallization event.

Hence it can be concluded that the kinetic process is complex mechanism in these systems and may not follow a single kinetic function. So to evaluate a single and invariant E throughout the process different isokinetic methods and isoconversional methods are needed to be applied.

References

[5.1] U. Koster U (1982) (B.L.Mordike, ed), Clausthal- Zellerfeld , DGM‘1983, pp.113-126.

[5.2] K. F. Kelton, A.L Greer. *J Non-Cryst Solids.* **79**; (1986):295.

[5.3] A.L Greer. *Mater.Sci.Eng.A* **179/180;** (1996):41.

[5.4] H.S Chen *J.Non-Cryst. Solids* **27;** (1978):257.

[5.5] M.C Weinberg. *Thermochim. Acta* **280/281;** (1996):63.

[5.6] J.S Blazquez, C.F Conde, A. Conde. *Acta Mater.* **53;** (2005):2305.

[5.7] H.E Kissinger. *Anal Chem.* **29;** (1957):1702.

[5.8] T. Ozawa. *Thermochim Acta* **100;** (1986):109.

[5.9] S. Mahadevan, A. Giridhar, A.K Singh. *J Non-Cryst Solids.* **88;** (1986):11.

[5.10] A.S Soltan. *Physica B.* **307**; (2001):78.

[5.11] N.J Afify. *Phys Chem Solids* **69;** (2008):1691.

[5.12] A.T Patel, A. Pratap. *J therm Anal Calorim.* **107;** (2012):159.

[5.13] J. Chovanee, M. Chromcikova, P. Pilny, J. Shanelova, J. Malek, M. Liska. *J Ther Anal Calorim.* **114;** (2013):971.

[5.14] K.N Lad, R.T Savalia, A. Pratap, G.K Dey, S. Banerjee. *Thermochim Acta.* **473;** (2008):74.

[5.15] N.M Abdelazim, A.Y Abdel-Latief, A.A Abu-Sehly, M.A Abdel-Rahim. *J Non Cryst Solids.* **387;** (2014):79.

[5.16] X.C Lu, H.Y Li. *J Them Anal Calorim.* **115;** (2014):1089.

[5.17] J. Wu, Y. Pan, J. Pi. *J Them Anal Calorim.* **115;** (2014):267.

[5.18] R. Svoboda, J. Malek. *J Therm Anal Calorim.* **115;** (2014):1961.

[5.19] S. Lesz, & D. Szewieczek, *Proceedings of the Worldwide Congress on Materials and Manufacturing Engineering and Technology COMMENT*, Poland, Gliwice-Wisla (CD-ROM), **637**; (2005):16.

[5.20] D. Szewieczek, & S. Lesz, *Proceedings of the 13th International Scientific Conference, Achievements in Mechanical & Materials Engineering AMME'05,* Gliwice-Wisla **637**; (2005): pp.

[5.21] D. Szewieczek, & S. Lesz, *J. Mater. Proces. Tech.* **157–158;** (2004):771.

[5.22] G.A. Jones, P. Bonnett & S.F.H. Parker, *J. Magnet. & Magnet. Mater.* **58;** (1986):216.

[5.23] D.M. Minic, & B. Adnadevic, *Thermochim. Acta* **474;** (2008):41.

[5.24] J.Malek. *Thermochim. Acta* **355;** (2000):239.

[5.25] D.M. Minic, A. Gavrilovic, P. Angerer, D.G. Minic, & A. Mariclc, *J. Alloy Comp.* **482**; (2009):502.

[5.26] F. Paulik. *Ch.10: Special Trends in Therm. Anal. John Wiley & Sons, Chichester, UK.* (1995).

[5.27] M.J. Starink, *J. Mater. Sci.* **32**; (1997): 6505.

[5.28] S. Vyazovkin and C.A. Wight, *The J. Phys. Chem.y A* **101;** (1997) :8279.

[5.29] S. Vyazovkin, C.A Wight. *Thermochim Acta.* **340-341;** (1999):53.

[5.30] A.K Burnham, L.N Dinh. *J Therm Anal Calorim.* **89(2);** (2007) :479.

[5.31] M.J Starnik. *Thermochim Acta.* **404;** (2003):163.

[5.32] S. Vyazovkin, D. Dollimore. *J Chem Inf Comput Sci.* **36(1);** (1996):42.

[5.33] A. Pratap, T.L.S Rao, K.N Lad, H.D Dhurandhar. *J Therm Anal Calorim.* **89(2);** (2007):399.

[5.34] T. Akahira, T. Sunose. *Research report (Chiba Institute of Technology). Sci Technol.* **16;** (1971):22.

[5.35] A.W Coats, J.P Redfern. *Nature (Lond).* **201;** (1964):68.

[5.36] A. Augis, J.E Bennett. *J Therm Anal Calorim.* **13;** (1978):283.

[5.37] P.G Boswell. *J Therm Anal Calorim.* **18;** (1980):353.

[5.38] T. Ozawa. *Bull Chem Soc Jpn.* **38;** (1965):1881.

[5.39] J.H Flynn, L.A Wall. *J Res Natl Bur Stand A Phys Chem* **70A**; (1966):487.

[5.40] C.D Doyle. *J Appl Polym Sci.* **5;** (1961):285.

[5.41] C.D Doyle. *J Appl Polym Sci.* **6;** (1962):642.

[5.42] C.D Doyle. *Nature(London).***207;** (1965):290.

[5.43] H.L Friedman. *J Polym Sci.* **C6**; (1964):183.

[5.44] Y.Q Gao, W. Wang. *J Non Cryst Solids.* **81;** (1986):129.

[5.45] A.N Kolmogorov. *Bull Acad Sci USSR Phys ser.* **3**; (1937):355.

[5.46] W.A Johnson, P.A Mehl. *Trans Am Inst Min Metall Eng.* **135;** (1939):416.

[5.47] M. Avrami. *J Chem Phys.* **7(12);** (1939):1103.

[5.48] M. Avrami. *J Chem Phys.* **8(2);** (1940):212.

[5.49] M. Avrami. *J Chem Phys.* **9(2);** (1941):177.

[5.50] N.S Mohan, R. Chen. *J Phys D Appl Phys*. **3;** (1970):243.

[5.51] W. Tang, Y. Liu, H. Zhang, C. Wang. *Thermochim Acta.* **408;** (2003):39.

[5.52] V.M Gorbachev. *J Therm Anal.* **8;** (1975):349.

[5.53] K. Matusita, S. Sakka. *Phys Chem Glasses.* **20;** (1979):81.

[5.54] W. Lu, B.Yan, W.H Huang. *J Non Cryst Solids.* **351**; (2005):3320.

[5.55] K. Matusita, S. Sakka. *J Non Cryst Solids.* **38-39**; (1980):741.

[5.56] D.W Henderson *J.Non-Cryst. Solids* **30**; (1979):301.

[5.57] J. Malek. *Thermochim Acta.***267; (**1995):61.

[5.58] J.Malek. *Thermochim Acta.* **355;** (2000):239.

[5.59] J. Sestak, G. Berggren. *Thermochim. Acta* **3;** 1971:1.

[5.60] F.J Gotor, J.M Criado, J. Malek, N. Koga. *J Phys Chem A.* **104;** (2000):10777.

[5.61] J.F Li, Z.H Huang, Y.H Zhou. *Intermetallics.* **15;** (2007):1013.

[5.62] J.Z Jiang, X.Y Zhuang, H. Rasmussen, J. Saida, A. Inoue. *Phys Rev B.* **64;** (2001):094208

[5.63] A.H Cai, W.K An, Y. Luo, T.L Li, X.S Li, X. Xiong, Y. Liu. *J Alloys Comp.* **490**; (2010):642.

[5.64] Y.L Gao, J. Shen, J.F Sun, G. Wang, D.W Xing, H.Z Xian, B.D Zhou. *Mater Lett.* **57;** (2003):1894.

[5.65] P.F Xing, Y.X Zhuang, W.H Wang, L. Gerward, J.Z Jiang. *J Appl Phys.* **91;** (2002):4956.

[5.66] J.S.C Jang, L.J Chang, G.L Chen, J.C Huang. *Intermetallics.* **13;** (2005):907.

[5.67] K.N Lad, R.T Savalia, A. Pratap, G.K Dey, S. Banerjee. *Thermochim Acta.* **473;** (2008):74.

[5.68] J.C Qiao, J.M Pelletier. *Trans Nonferrous Met Soc China.* **22;** (2012):577.

[5.69] K.G Prashanth, S. Scudino, K.B Surreddi, M. Sakaliysa, B.S Murty, J. Eckert. *Mater Sci Eng A.* **513-514;** (2009):279.

[5.70] X. Lu, H. Li, P. Xiao, R. Wu, D. Li. *Thermochim Acta.* **570;** (2013):27

[5.71] S. Kasyap, A. Patel, A. Pratap. *J Ther Anal Calorim.* **116;** (2014):1325.

[5.72] A.T Patel, A. Pratap. *J therm Anal Calorim.* **107;** (2012):159.

[5.73] G.P Johari, J.W.P Schmelzer. *Schmelzer JWP (Ed) Glass: Selected Properties and Crystallization. Walter de Gruyter & Co;* (2014):521.

[5.74] Y. X Zhuang, T.F Duan, H.Y Shi. *J Alloys Compd.* **509;** (2011):9019

[5.75] A.P Srivastava, D. Srivastava, B. Mazumdar, G.K Dey. *J Ther Anal Calorim.* **119**; (2015):1353.

[5.76] Z. Zhang, W.H Wang, Y. Hirotsu. *Mater Sci Engg A.* **385;** (2004):38.

[5.77] M. Lasocka. *Mater Sci Eng.* **23;** (1975):173.